Food Chemistry 438 (2024) 137935

Contents lists available at ScienceDirect

Food Chemistry

journal homepage: www.elsevier.com/locate/foodchem

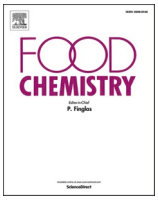

Kinetics of aroma formation from grape-derived precursors: Temperature effects and predictive potential

Elayma Sánchez-Acevedo, Ricardo Lopez *, Vicente Ferreira

Laboratory for Flavor Analysis and Enology (LAAE), Department of Analytical Chemistry, Faculty of Sciences, Universidad de Zaragoza, Instituto Agroalimentario de Aragón-IA2 (Universidad de Zaragoza-CITA), Associate Unit to Instituto de las Ciencias de la Vid y del Vino (ICVV) (UR-CSIC-GR), E-50009 Zaragoza, Spain

ARTICLE INFO

Keywords:
Grapes
Wine aroma
Aroma formation
Aroma precursors
Acid hydrolysis
Wine aging

ABSTRACT

This study investigates the accumulation and degradation of aroma molecules released by acid hydrolysis of aroma precursors in winemaking grapes. A first-order kinetics model effectively interprets this accumulation, including subsequent degradation. Experimentation at three temperatures categorizes specific grape-derived aroma molecules into three stability-based groups: labile molecules from labile precursors, stable molecules from labile precursors, and stable molecules from stable precursors. While many grape-derived aromas exhibit similar patterns and levels of accumulation across temperatures, reaction rates significantly increase with temperature. The analysis of 12 samples of two grape varieties hydrolyzed at 50 °C for 5 weeks and 75 °C for 24 h confirms that fast hydrolysis accurately replicates varietal and between-sample aroma compositional differences. Moreover, the accumulated levels of 21 relevant grape-derived aromas strongly correlate with those at 50 °C, indicating that fast hydrolysis at 75 °C reliably predicts grape aroma potential.

1. Introduction

Aroma is one of the most important characteristics defining wine quality and acceptability. A significant and particularly appreciated part of wine aroma is related to the grape and it is usually known as varietal aroma. Against old beliefs, varietal aroma is not limited to what enologists traditionally have known as primary aroma, which encloses just the aroma molecules already present in grapes (Bakker & Clarke, 2011). Instead, wine varietal aroma should include all aroma molecules whose main carbon chain was synthetized in the grape and that, by a series of relatively simple chemical processes, such as hydrolysis, dehydration, cyclation, or esterification, form the aroma molecule at some time of wine production and storage (Ferreira & Lopez, 2019). Since these processes can take long times, a significant part of wine varietal aroma has been traditionally classified as "tertiary aroma" or "aroma of evolution" or "aging bouquet" (Bakker & Clarke, 2011). This is particularly evident in the neutral grapes most often used for producing dry wines. In these grapes most aroma compounds are present as nonvolatile precursors, including polyolic forms (Williams et al., 1980), cysteinylated, glutathionylated, cysteinyl-glycine conjugated and glutamyl-cysteine conjugated precursors (Bonnaffoux et al., 2018; Cibaka et al., 2017; Tominaga et al., 1998), dimethyl sulfide (DMS) precursors (Segurel et al., 2005) and glycosidic precursors (Hjelmeland & Ebeler, 2015).

The relevance of this pool of aroma compounds on wine aroma was demonstrated in some old reports revealing the existence of a connection between the aromatic quality of wine and the aroma precursor content in grapes (Francis et al., 1992).

Different methods for the isolation and quantitative assessment of the pool of aroma precursors have been developed with time. Some authors, aiming mainly to understand the nature of the aglycone part of the glycosidic precursors, have preferred enzymatic hydrolysis of the precursor fraction (Schneider et al., 2001). The limitation of this approach is that it cannot provide a reliable assessment of the aroma potential, since many aroma molecules derived from precursors are not present as aglycones, but derive from the chemical transformation of the aglycone. This is particularly evident for norisoprenic precursors, such as β -damascenone or TDN (Strauss et al., 1986). For assessing these types of aroma volatiles, acid hydrolysis is preferred (Loscos et al., 2009; Slaghenaufi & Ugliano, 2018; Williams et al., 1989). For quantitative purposes, a fast hydrolysis at 100 °C has been often used (Ibarz et al., 2006; Loscos et al., 2009). However, in these harsh conditions, labile aroma molecules, such as linalool and geraniol, are quickly degraded (Hampel et al., 2014), and the hydrolyzed models display poor odor nuances. Better aromatic properties are derived if the hydrolysis of the

* Corresponding author.
E-mail addresses: esanchezacevedo@unizar.es (E. Sánchez-Acevedo), riclopez@unizar.es (R. Lopez), vferre@unizar.es (V. Ferreira).

https://doi.org/10.1016/j.foodchem.2023.137935
Received 28 June 2023; Received in revised form 12 October 2023; Accepted 3 November 2023
Available online 8 November 2023

fraction of precursors is carried out at mild temperatures as demonstrated by Francis et al (Francis et al., 1992). However, some aroma descriptors developed during hydrolysis of purified precursor extracts, such as honey or tea (Francis et al., 1992; López et al., 2004), suggest that oxidation and thermal degradation processes occur under these conditions. Part of this oxidation can be avoided if the hydrolysis is carried out in complete anoxia (Oliveira & Ferreira, 2019) and, particularly, if the extract is not purified and includes grape or wine polyphenols (Alegre, Arias-Pérez, et al., 2020). Under these conditions, even at 75 °C, reliable sensory profiles congruent with the olfactory nuances of unoxidized wine and related to grape variety, are obtained (Alegre, Sáenz-Navajas, et al., 2020). This suggests that this fast hydrolysis could be a promising tool for the study of the aroma potential in winemaking grapes.

Some works report data about the evolution with time of aroma compounds produced by the hydrolysis of aroma precursors extracted from grapes (Denat et al., 2022; Oliveira & Ferreira, 2019). More recently, there are similar reports in wine aged in bottles at room temperature (Vázquez-Pateiro et al., 2020) or at 50 °C (Carlin et al., 2022) and 60 °C (Slaghenaufi & Ugliano, 2018). All these works demonstrate that the different aroma molecules follow quite different patterns of hydrolysis with time, from labile aroma molecules such as linalool and geraniol, which quickly reach a maximum and their levels further decay (Oliveira & Ferreira, 2019; Slaghenaufi & Ugliano, 2018) to stable aroma molecules, such as TDN, which seem to increase continuously throughout aging (Carlin et al., 2022; Oliveira & Ferreira, 2019).

However, most of these reports consider a limited number of sampling points or do not make it possible to compare between different temperatures. This makes that the nature of the kinetics of aroma accumulation during aging and the effects of temperature on those kinetics remain unclear. Therefore, the main objective of this research is to compare the kinetics of the accumulation of aroma molecules derived from grape precursors at three different temperatures. A secondary objective is to assess whether fast hydrolysis conditions (24 h at 75 °C) correlates with the hydrolysis obtained in mild conditions (5 weeks at 50 °C), which would be essential to develop reliable field assays for assessing grape aroma potential.

2. Material and methods

2.1. Reagents and standards

ACS quality absolute ethanol was obtained from Panreac (Barcelona, Spain), pure water was purchased from a Milli-Q purification system (Millipore, USA) and LiChrosolv quality. HPLC quality methanol was obtained from Merck (Darmstadt, Germany). Sep Pak C18 silica, prepacked in 10 g cartridges were obtained from Waters (Ireland). A VAC ELUT 20 station supplied by Varian (Walnut, Creek, USA) was used to perform the semiautomated solid phase extraction (SPE). L-tartaric acid was supplied by Panreac (Barcelona, Spain).

2.2. Grape samples and phenolic and aromatic fractions (PAFs)

PAFs were obtained from ethanolic must (mistelle) according to the procedure described by Alegre, Arias-Pérez, et al. (2020). For the preparation of mistelles, the grapes were first destemmed and crushed in the presence of 15% (p/p) of ethanol and 5 g/hL of potassium metabisulfite (Merck, Germany). After 7 days of maceration at 13 °C, the mistelles were pressed, filtered and stored at 5 °C in the dark. For the obtention of PAFs, according to the procedure, first 750 mL of mistelle were dealcoholized in a rotatory evaporator to a final volume of approximately 410 mL containing less than 2% (v/v) ethanol. This volume was percolated through a 10 g prepacked Sep Pak C18 cartridge (previously conditioned with methanol followed by milli-Q water with 2% of ethanol). Sugars, amino acids, acids and ions were removed by washing with milli-Q water at pH 3.5. The cartridge was dried by letting air pass through and the polyphenolic and aromatic precursor fraction (PAF) was recovered by elution with 100 mL of absolute ethanol.

The study was carried out with a total of 12 PAFs (6 of Grenache (G) and 6 of Tempranillo (T) grapes) obtained with ripening grapes from different producers of north Spain. Specifically, samples G1, G4, T3, T4, T5 and T6 were collected from different vineyards of Bodegas Ramon Bilbao. Samples G2, G3 and T1 were obtained from Bodegas y Viñedos Ilurce. These last wineries are from D.O.Ca. La Rioja. Samples G5 and G6 came from Viñas del Vero in D.O. Somontano and sample T2 was obtained from Dominio Pingus in D.O. Ribera del Duero.

2.3. Acid hydrolysis of PAFs

After carried out the process described in Section 2.2, each PAF was reconstituted as described by Alegre, Arias-Pérez, et al. (2020) to 100 mL with water containing 5 g/L of tartaric acid to form a model wine (rPAF) with 13.3% (v/v) ethanol and pH adjusted to 3.5. Then, the reconstituted PAFs were introduced into the anoxic chamber Jacomex P [Box] (Dagneux, France) and distributed into headspace vials with screw top (Merck, Germany) which were closed within the chamber and were further bagged into two consecutive thermo-sealed plastic bags. The bags were of certified oxygen permeability and contained activated charcoal with an oxygen scavenger (AnaeroGen from Thermo Scientific Waltham, Massachusetts, United States).

In the first part of this work (evaluation of kinetics liberation of aroma compounds) two samples of Grenache (G1 and G2) were evaluated. Both samples were hydrolyzed at 35 °C (1.5, 3.5, 6 and 9 months), at 50 °C (3.5, 7, 14, 35, 49, 70 and 98 days) and at 75 °C (1, 2, 6, 24, 48 and 96 h). In the second part, 12 samples (6 of Grenache and 6 of Tempranillo grapes) were evaluated at two points in time: at 75 °C for 24 h (fast hydrolysis) and at 50 °C for 5 weeks (mild hydrolysis). All samples were prepared in replicates and analyzed independently.

2.4. Quantification of aroma released by acid hydrolysis

The aroma compounds released by acid hydrolysis were analyzed by three analytical methods. A first one specifically suited for Strecker aldehydes (isobutanal, 2-methylbutal, isovaleraldehyde, methional, phenylacetaldehyde), a second one for varietal thiols (3-mercaptohexanol, 4-mercapto-4-methylpentan-2-one and 3-mercaptohexyl acetate) and a third one for minor and trace aroma compounds, which includes volatile compounds no analyzed by the previous methods.

2.4.1. Analysis of minor and trace volatile compounds by GC–MS

The method for the extraction of volatile compounds released by acid hydrolysis, was carried out as described by López et al. (López et al., 2002). For this purpose, 15 mL of PAF hydrolysate added with 2-octanol, 3-octanone and 3,4-dimethylphenol as internal standards were summited to a solid phase extraction and 2 μL of the obtained extract was injected in a system GC–MS for the quantification of aroma compounds following the chromatographic method proposed by Oliveira et al. (Oliveira & Ferreira, 2019).

2.4.2. Analysis of Strecker aldehydes by GC–MS

Strecker aldehydes were analyzed following the method optimized and validated by Castejón-Musulén et al. (Castejón-Musulén et al., 2022). According to that method, 12 mL of PAF hydrolysate, added with 2-methylpentanal, 3-methylpentanal, methional-d_3, phenyl-d_5-acetaldehyde as internal standards, were derivatized under anoxia with O-(2,3,4,5,6-pentafluorobenzyl)hydroxylamine into their corresponding oximes, followed by a solid phase extraction and analysis by GC–MS.

2.4.3. Analysis of varietal thiols by UHPLC-QqQ-MS

The method used for determination of polyfunctional mercaptans was the one proposed by Vichi et al. (Vichi et al., 2015). The method consisted of a single-step derivatization/extraction procedure of 10 mL

of PAF (added with d_5-3-mercaptohexanol, d_{10}-4-mercapto-4-methylpentan-2-one and d_5-3-mercaptohexyl acetate as internal standards) hydrolysate followed by UHPLC-QqQ-MS analysis using ebselen (Sigma–Aldrich, USA) as a derivatization agent. The mechanism of the ebselen–thiol reaction consists of the cleavage of the Se-N bond of ebselen by the SH group of the thiol and the formation of the corresponding selenenyl sulfide Se-S bond.

2.5. First order kinetic models to interpret experimental C vs time plots

2.5.1. Stable aroma molecules

If the aroma molecule is stable and there are no degradation processes, the evolution with time of the concentration of the aroma molecule formed by the hydrolysis of a precursor will follow mathematical functions of the type:

$$C_a^t = C_p^o \cdot (1 - e^{-k_h t})$$

where C_a^t is the concentration of the aroma molecule at time t; C_p^o is the concentration of the aroma precursor at the beginning (time 0), k_h is the kinetic constant of the hydrolysis of the precursor and t is the time. Plots of this type can be seen in Fig. S1 of the supplementary material.

These plots have the property that the representation of the natural logarithm of $\left(1 - C_a^t/C_a^o\right)$ vs. time is a straight line whose slope is -k_h. In the cases in which there are several precursors differing in concentration and in the kinetic hydrolysis constants, those representations may turn not to be linear anymore, particularly if the differences between hydrolyses constants are large.

2.5.2. Unstable aroma molecules

If the aroma molecule is unstable and reacts with water or another wine component, then the evolution with time will be the combination of the process of hydrolysis of precursor and that of the degradation of the aroma molecule. Here, as a first approximation, we will also assume that aroma degradation processes follow 1st order kinetics -case of spontaneous hydrolysis or molecular rearrangement of the molecule, or pseudo 1st order kinetics -case of reaction to other wine components. In the case of pseudo 1st order kinetics, the hydrolysis constants will differ between wines. The degradation will follow the law:

$$C_a^t = C_a^o \cdot e^{-k_d t}$$

where C_a^t is the concentration of aroma molecule at time = t, C_a^o is the initial concentration of the aroma molecule, and k_d is the kinetic constant of the degradation process.

The combination of hydrolysis and degradation processes makes it possible to estimate the plots representing the amounts of accumulated aroma molecule versus time.

For that, the amount of aroma molecule produced by hydrolysis of the precursor at time t is:

$$-dC_p^t = dC_{a(hyd)}^t = C_p^t \cdot k_h \cdot dt$$

While the amount of aroma molecule degraded at that time point is:

$$-dC_{a(\mathrm{deg})}^t = C_a^t \cdot k_d \cdot dt$$

Then, by differential analysis or by using a spreadsheet it is possible to generate different types of plots attending to the relative magnitudes of the hydrolysis and degradation kinetic constants. Some of these representations are given in the Fig. S2 of the Supplementary material, in which there is also a short tutorial explaining how the combined functions were obtained using an Excel spreadsheet (Fig. S3 of the supplementary material).

3. Results and discussion

3.1. Evolution of aroma compounds at three different temperatures

Extracts from two different samples of Grenache grapes (G1 and G2) were hydrolyzed in complete anoxia at three different temperatures: 35, 50 and 75 °C. Samples at 35 °C were taken for 9 months, at 50 °C for 98 days (3.2 months) and at 75 °C for 96 h. To facilitate interpretation, and to assess the relationship between reaction rates at the different temperatures, the plots at 35 and 50 °C of some selected compounds displaying clearly identifiable maxima or plateaus at the three temperatures were rescaled so that, in average, the plots were superimposable to those obtained at 75 °C (Raw data are available in Tables S1 and S2). Compounds used to make the fits were linalool, geraniol, Riesling acetal, α-terpineol and β-damascenone, and the best compromise solution was obtained when 21.7 days at 50 °C and 5.0 months at 35 °C equal 50 h at 75 °C. All plots shown in Figs. 1 to 3 are represented using this time scale.

These scale factors provide a first approximation of the relationships between the reaction rates at the three temperatures. Based on their values, it can be roughly estimated that the reaction rates increase by factors of 6.9 and 72 when the temperature increases from 35 to 50 or 75 °C, respectively. If the natural logarithms of these factors are then represented versus 1/T, where T is the corresponding absolute temperature, the regression line of the Arrhenius-like plot obtained has a determination coefficient $R^2 = 0.997$, significant at $P < 0.05$, which makes it possible to establish that, roughly and in general, the chemical processes related to the accumulation of the selected aroma molecules from the hydrolysis of specific precursors are at 75 °C, slightly more than 460 times faster than at 20 °C, and at 50 °C, approximately 37 times faster and at 35 °C 6.5 times faster than at 20 °C.

As it is obvious from the comparison of the plots at the three temperatures, sampling times are not equivalent at the three temperatures. Those at 50 °C were, relatively, the longest, so this temperature has been preferably used to set the evolution pattern of the different compounds.

In order to interpret the different plots C vs t given in Figs. 1-3, there are some basic aspects to consider. First, that aroma molecules are formed from different specific aroma precursors through a series of spontaneous processes at wine pH. Some of the aroma molecules are itself unstable or quite reactive, so that when monitoring the evolution with time of the concentration of aroma molecules derived from aroma precursors, the outcome may not represent just the reaction through which the aroma molecule is formed, which will be herein referred to as the hydrolysis process, but the combination of this reaction with all those others in which the aroma molecule could be further involved, which will be herein referred to as the degradation process. As a first approximation, both reactive processes have been interpreted through first order kinetics, as detailed in the material and methods Section 2.5 and in the supplementary material (Figs. S1-S3). The critical parameters governing those models are the corresponding kinetic constants: k_h for the hydrolysis of the precursor and k_d for the degradation of the aroma molecule. Typical plots obtained using different combinations of k_h and k_d values are given in Figs. S1 and S2 of the supplementary material and used to discuss the experimental results.

Based on all previous considerations, aroma molecules derived from specific precursors can be classified into three different basic categories, with the last one further subdivided into another three subcategories:

1. Labile aroma molecules (k_d large) derived from labile precursor molecules (k_h large).
2. Stable aroma molecules (k_d small) derived from labile precursor molecules (k_h large)
3. Stable aroma molecules (k_d small) derived from rather stable precursor molecules (k_h small). Here, three different subcategories emerge attending to the role played by temperature:
   a. Small; the previous kinetic considerations roughly apply.

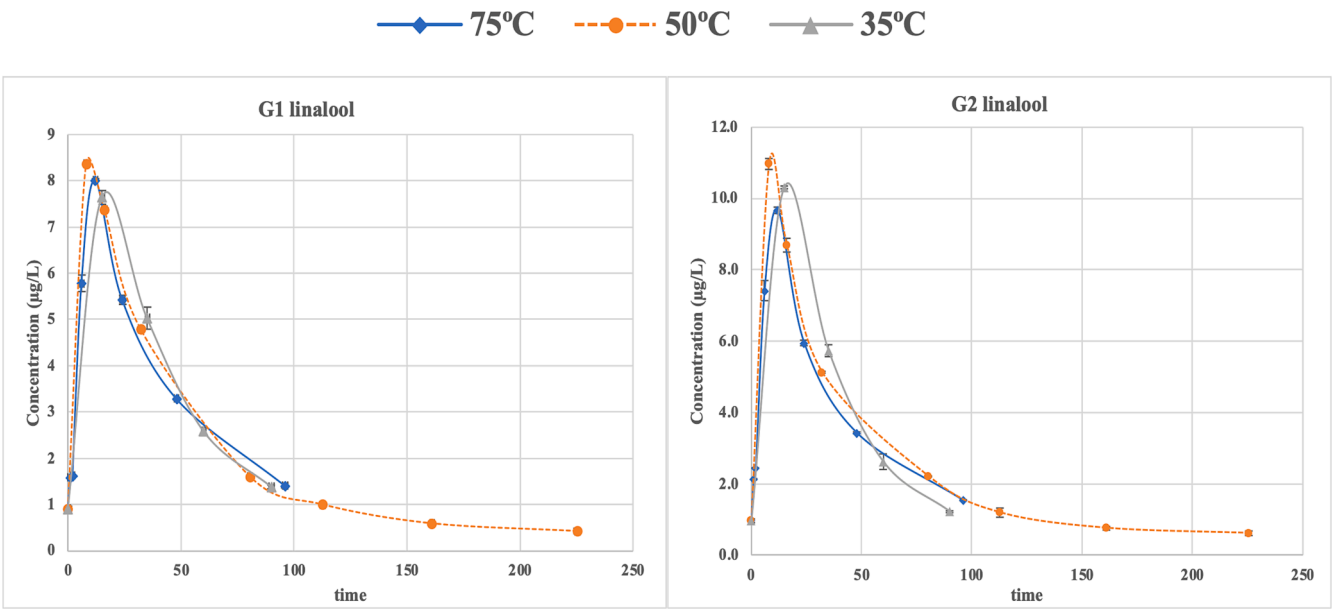

Fig. 1. Evolution with time of the levels of linalool during the anoxic incubation of two wine models containing polyphenolic and aromatic extracts from two different lots of Grenache grapes. To facilitate comparison, time scales have been normalized. Data at 75 °C are expressed directly in hours, those at 50 °C, divided by 2.3 are days (the 100 coordinate = 43.5 days), and those at 35 °C, divided by 10 are months (the 50 coordinate = 5.0 months). Error bars represent standard error of the means.

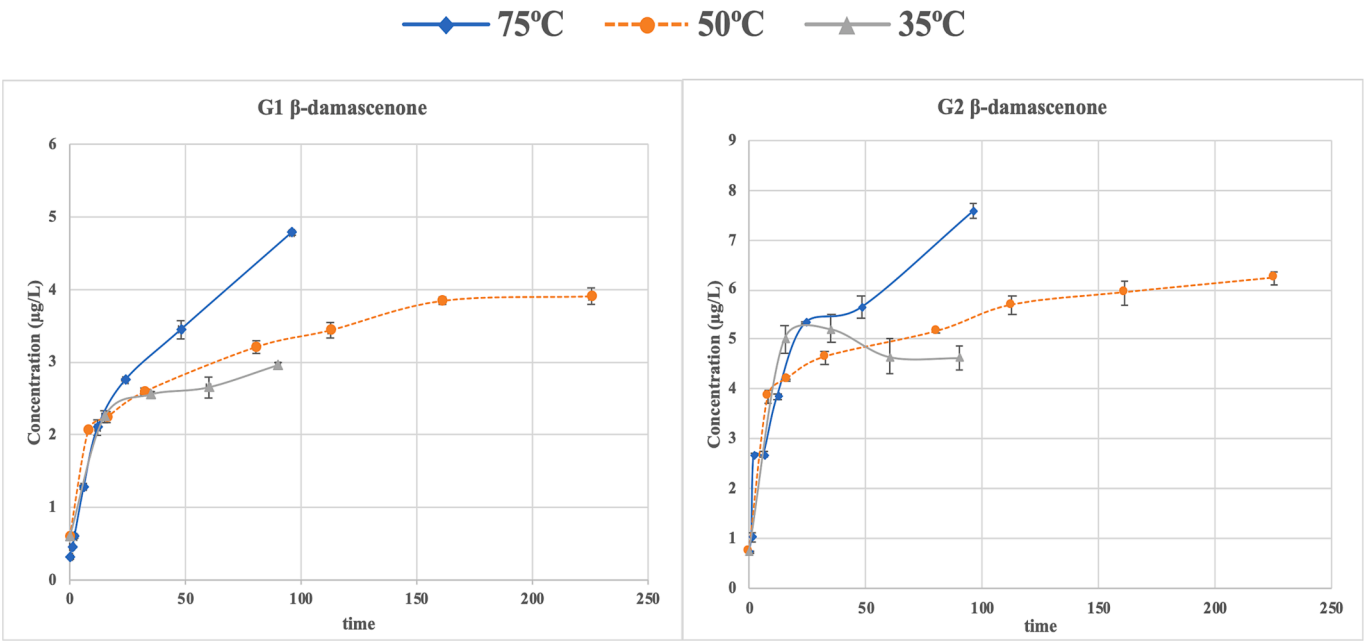

Fig. 2. Evolution with time of the levels β-damascenone during the anoxic incubation of two wine models containing polyphenolic and aromatic extracts from two different lots of Grenache grapes. To facilitate comparison, time scales have been normalized. Data at 75 °C are expressed directly in hours, those at 50 °C, divided by 2.3 are days (the 100 coordinate = 43.5 days), and those at 35 °C, divided by 10 are months (the 50 coordinate = 5.0 months). Error bars represent standard error of the means.

b. Moderate; the previous kinetic considerations are no longer valid.
c. Extreme; at 35 °C the reactions nearly do not take place.

In the following subsections, the different patterns will be presented and discussed.

3.1.1. Labile aroma molecules (k_d large) derived from labile precursor molecules (k_h large)

These are geraniol, linalool, Riesling acetal and α-terpineol. Fig. 1 shows linalool as an example (the other compounds can be found in Fig. S4 of the supplementary material). As can be seen, the evolutions of these four aroma components were characterized by the presence of a maximum, although in the cases of Riesling acetal and α-terpineol, the maxima could be clearly observed only in the plot at 50 °C. These patterns are characteristic of labile aroma compounds derived from labile precursor molecules as can be seen in Fig. S2 in the supplementary material. In the cases of linalool and geraniol, the maxima were observed in the first sampling points taken at 35 and 50 °C (1.5 months

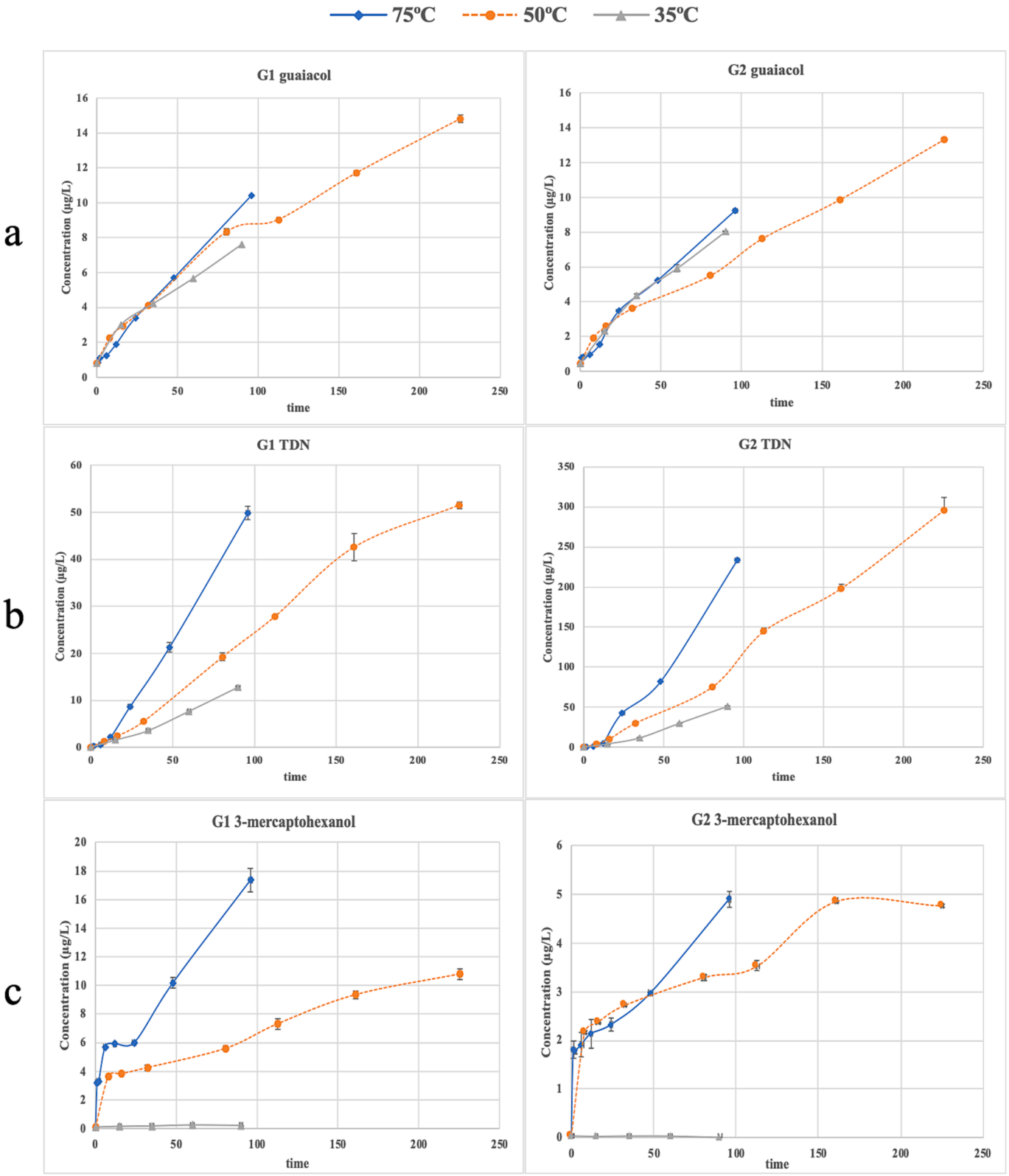

Fig. 3. Evolution with time of a: guaiacol, b: TDN and c: 3-mercaptohexanol, during the anoxic incubation of two wine models containing polyphenolic and aromatic extracts from two different lots of Grenache grapes. To facilitate comparison, time scales have been normalized. Data at 75 °C are expressed directly in hours, those at 50 °C, divided by 2.3 are days (the 100 coordinate = 43.5 days), and those at 35 °C, divided by 10 are months (the 50 coordinate = 5.0 months). Error bars represent standard error of the means.

and 3.5 days, respectively), in agreement with earlier reports (Williams et al., 1980). Only at 75 °C sampling points were enough to locate with precision the maxima, which was found in both cases at the third sampling point (12 h). The plots obtained for these two compounds were similar to the third one provided in Fig. S2 (obtained with $k_h = 5$ and $k_d = 5$), which corresponds to very fast hydrolysis and degradation processes, which is consistent with the results of Carlin et al. (Carlin et al., 2022). Riesling acetal and α-terpineol reached the maxima significantly later, at the 6th sampling point at 75 °C (25.7 h), the 4th at 50 °C (14 days) and the 4th or 5th at 35 °C (6 or 9 months), although at this temperature the maxima were not clearly observed. The plots of both compounds were similar to those in the middle of Fig. S2 (obtained with $k_h = 1$ and $k_d = 1$), which suggests that for these two compounds both the hydrolysis of the precursor and the degradation of the molecule were slower chemical reactions than those of linalool and geraniol.

Interestingly, in the case of α-terpineol, there was a marked effect of temperature on the accumulation of aroma molecule. Maxima levels were in both samples observed at 75 °C, and minima levels at 35 °C. As sampling points at 35° and 75 °C had not been enough to completely observe the decay of the concentrations at longer times it was not possible to make a precise diagnose of the reason for this. As shown in Fig. S2, aroma molecules accumulate more if hydrolysis constants are higher and aroma degradation molecules are smaller. Based on this observation, it could be thought that higher temperatures have a greater effect on the reaction of hydrolysis of the precursor than on the reaction of degradation of the aroma molecule. However, α-terpineol is also known to be a by-product of the degradation of other terpenes (Maicas & Mateo, 2005) so that the specific temperature dependence of this compound could be well explained because at higher temperatures there was a higher level of degradation of other terpenes. Such higher degradation is, however, not observed for linalool and geraniol.

3.1.2. Stable aroma molecules (k_d small) derived from labile precursor molecules (k_h large)

This group includes two norisoprenoids: β-damascenone and vitispirane and two phenylpropanoids: vanillin and acetovanillone. Fig. 2 shows the evolution of β-damascenone and the rest of these four aroma molecules is shown in Fig. S5 of the supplementary material. It is noteworthy that in the two norisoprenoids, the aroma molecules accumulated at slightly but significantly higher levels at 75 °C, which could be related to the known fact that these aroma compounds are products of carotenoid breakdown (Daniel et al., 2008). Even though the plateaus were not clearly observed, all the plots had maximum accumulation rates at the first sampling points and the rates of accumulation progressively decreased; thus, it can be suggested that in all the cases the plots are similar to those reported in Fig. S1, related to stable compounds derived from the hydrolysis of precursor molecules. β-damascenone has been reported to be degraded in the presence of SO_2 (M. A. Sefton et al., 2011), but this antioxidant was not present in the wine models. The existence of plateaus in the evolutions of β-damascenone and vitispirane has been previously observed (Carlin et al., 2022; Slaghenaufi & Ugliano, 2018).

3.1.3. Stable aroma molecules (k_d small) derived from rather stable precursor molecules (k_h small)

(a) Stable aroma molecules (k_d small) derived from stable precursor molecules (k_h large) with small temperature effects

The compounds in this category are guaiacol, whose evolution over time is shown in Fig. 3a, ethyl cinnamate and massoia lactone, whose evolution patterns are shown in Fig. S6 of the supplementary material. At least in these two last cases, the formation pathways include more steps than the hydrolysis of a glycosidic precursor. Ethyl cinnamate is formed by esterification of cinnamic acid with ethanol, and cinnamic acid comes at least in part from a glycosidic precursor. In fact, two glycosides of cinnamic acid have been found in wine made from Korean black raspberries (Cho et al., 2014). Massoia lactone in turn is formed through the internal esterification of the corresponding γ-hydroxyacid. Considering that several glycosidic precursors of the structurally equivalent whiskylactones have been described in oak wood (Hayasaka et al., 2007; Wilkinson et al., 2013) glycosides of the hydroxyacid precursor to massoia lactone may also exist. Finally, guaiacol is produced by the hydrolysis of a glycosidic precursor as described by Hayasaka et al. (Hayasaka et al., 2010); also, acid hydrolysis of wines and berries resulted in a several-fold increase in free guaiacol (Singh et al., 2011).

(b) Stable aroma molecules (k_d small) derived from stable precursor molecules (k_h large) with moderate temperature effects

The compounds in this category are TDN (Fig. 3b), syringol, linalool oxide and methoxyeugenol, whose evolution over time followed the patterns given in Fig. S7 of the supplementary material. The first three molecules are very different in chemical structures and in biochemical origin. TDN is a norisoprenoid, methoxyeugenol and syringol are vanillin relatives (phenylpropanoid) and linalool oxide is a terpene. In all cases glycosidic precursors have been previously described (Coulter et al., 2022; Schievano et al., 2013).

The four aroma compounds in this category have in common that they seem to be the endpoint of complex chemical degradation routes of the three different families of components: norisoprenoids, phenylpropanoids and terpenes. This would be in agreement with their continuous accumulation, with no evidences suggesting that the accumulation rates decrease. Temperature effects were more or less evident in all cases, and in general, revealed higher accumulation rates at higher temperatures, which suggests that the reactions through which these compounds are produced, had much higher energies of activation than those through which compounds in the previous categories were produced, most of them hydrolysis of glycosidic bonds.

(c) Stable aroma molecules (k_d small) derived from stable precursor molecules (k_h large) with extreme temperature effects

Three compounds belong to this category: 4-vinylguaiacol, 4-vinylphenol (Fig. S8 of the supplementary material) and 3-mercapthexanol (MH), whose evolution over time followed the patterns given in Fig. 3c. As can be seen, the most outstanding feature of the evolutions of these compounds was the strongest temperature effect. Leaving aside MH in G2, in all the five other cases, the rates of aroma accumulation at 75 °C were much higher, and in the six cases, the rates of accumulation of the aroma compound at 35 °C were simply residual in comparison to those observed at higher temperatures. This strongly suggests that the activation energy of the hydrolysis reactions of the corresponding precursors was large, so that high temperatures were required to cleave the precursor. This would have been expected in the case of the different precursors of MH, in which a thioether C—S bond has to be cleaved. In the cases of vinylphenols this explanation is less convincing, since the precursors for these compounds are expected to be glycosides whose cleavage should not be much different than those of the other phenols measured in this work, such as syringol, methoxyeugenol, vanillin or guaiacol for which the effects of the temperature were much weaker. Therefore, it can be speculated that other reactions may be taking place. Vinylphenols are reactive compounds with a strong electrophilic character. These compounds are known to react to nucleophiles such as mercaptans (Naim et al., 1993), and are also known to react to anthocyanins to form pyranoanthocyanins (Hillebrand et al., 2004). It can then be hypothesized that the poor accumulation of these compounds at low temperatures may also be due, in part, to a competitive reaction with anthocyanins, which at high temperature would be involved in other reactions such as the thermal decarboxylation of p-coumaric and ferulic acids to produce the correspondent vinylphenols (Tambawala et al., 2022).

3.2. Can fast hydrolysis at 75 °C predict grape aroma potential?

In the second part of this study, wine models containing PAFs extracted from 12 different batches of ripened winemaking grapes from Grenache and Tempranillo varieties were hydrolyzed in complete anoxia at 75 °C for 24 h (fast hydrolysis) and at 50 °C (mild hydrolysis) for 5 weeks. Fast hydrolysis has been recently proposed and used to assess the aroma potential of samples from these varieties with apparently good results (Alegre, Sáenz-Navajas, et al., 2020). However, although it was previously compared with the mild hydrolysis at 50 °C (Alegre, Arias-Pérez, et al., 2020), the comparison was based on a quite limited number of samples and did not include all relevant analytes. In the present case, 25 volatile compounds were determined using three different analytical procedures and the results are summarized in Tables 1 and 2.

3.2.1. Varietal and hydrolysis differences. Principal component analysis (PCA)

Fig. 4 summarizes the results of Principal Component Analysis (PCA) of the volatile compounds quantified in this experiment. In the plane formed by the first two principal components, which accumulates 62% of the original variance, samples are majorly distributed by grape variety, with samples from Grenache on the right and those from Tempranillo, except T5, on the left.

As can be seen, Grenache samples were characterized by larger quantities of TDN, massoia lactone, vinyl phenols, Strecker aldehydes and terpenols, while those from Tempranillo contained higher amounts of phenols. Results about thiols confirmed that 3-mercaptohexanol is a normal constituent of hydrolysates at 50 and 75 °C and that it was found at higher levels in hydrolysates from Grenache, which agrees with the known role that this compound has been found to play in Grenache rosé wines (Ferreira et al., 2002). It can be also observed that little amounts of three Strecker aldehydes: 3-methylbutanal, methional and

Table 1
Average concentrations and standard deviations (n = 2) of the aroma compounds (expressed in μg/L) evaluated at two different conditions (5 weeks at 50 °C and 24 h at 75 °C) in the 6 PAFs of Grenache. (n.d.: the compound was not detected).

Compounds	G1		G2		G3		G4		G5		G6	
	50 °C	75 °C	50 °C	75 °C	50 °C	75 °C	50 °C	75 °C	50 °C	75 °C	50 °C	75 °C
3-mercaptohexanol	5.59 ± 0.16	6.00 ± 0.08	3.29 ± 0.06	2.32 ± 0.14	5.11 ± 0.08	5.21 ± 0.02	18.2 ± 0.3	16.8 ± 1.2	19.6 ± 0.6	20.1 ± 0.2	17.1 ± 0.3	17.1 ± 1.9
isobutanal	1.76 ± 0.02	1.31 ± 0.02	2.09 ± 0.03	1.89 ± 0.19	1.16 ± 0.06	1.30 ± 0.03	1.81 ± 0.18	2.16 ± 0.07	2.56 ± 0.07	2.91 ± 0.15	1.95 ± 0.13	2.21 ± 0.10
2-methylbutanal	2.63 ± 0.16	2.86 ± 0.14	3.58 ± 0.08	3.19 ± 0.24	3.11 ± 0.15	2.80 ± 0.16	3.60 ± 0.20	4.08 ± 0.25	3.72 ± 0.03	3.68 ± 0.09	3.21 ± 0.19	3.47 ± 0.21
isovaleraldehyde	2.16 ± 0.08	2.55 ± 0.01	1.93 ± 0.07	2.44 ± 0.05	1.72 ± 0.06	2.27 ± 0.02	2.82 ± 0.10	4.37 ± 0.17	4.21 ± 0.04	5.28 ± 0.01	1.97 ± 0.05	2.68 ± 0.03
methional	1.34 ± 0.04	2.11 ± 0.11	1.49 ± 0.05	2.30 ± 0.12	n.d.	1.72 ± 0.06	0.961 ± 0.042	1.76 ± 0.07	1.01 ± 0.05	1.82 ± 0.01	0.66 ± 0.03	1.59 ± 0.03
phenylacetaldehyde	5.98 ± 0.29	6.65 ± 0.22	5.28 ± 0.03	9.98 ± 0.04	1.65 ± 0.04	2.80 ± 0.11	2.63 ± 0.06	7.40 ± 0.30	1.60 ± 0.04	4.46 ± 0.05	1.26 ± 0.07	3.61 ± 0.05
γ-nonalactone	0.894 ± 0.012	0.782 ± 0.008	0.960 ± 0.019	0.923 ± 0.016	0.583 ± 0.037	0.527 ± 0.012	1.02 ± 0.02	0.887 ± 0.009	1.37 ± 0.06	0.890 ± 0.002	1.28 ± 0.18	1.20 ± 0.02
massoia lactone	3.10 ± 0.11	1.92 ± 0.02	2.62 ± 0.09	1.89 ± 0.02	6.22 ± 0.29	6.08 ± 0.15	8.91 ± 0.14	8.05 ± 0.01	4.67 ± 0.08	4.35 ± 0.09	51.6 ± 0.1	60.6 ± 2.5
β-damascenone	3.21 ± 0.09	2.75 ± 0.01	5.15 ± 0.06	5.33 ± 0.18	9.95 ± 0.65	9.76 ± 0.41	3.86 ± 0.01	3.40 ± 0.01	3.46 ± 0.11	2.83 ± 0.1	10.0 ± 0.12	13.2 ± 0.1
Riesling acetal	7.86 ± 0.25	4.92 ± 0.04	26.8 ± 1.0	18.4 ± 0.1	20.7 ± 0.7	11.2 ± 0.3	20.8 ± 0.4	13.8 ± 0.2	34.5 ± 0.8	24.0 ± 0.4	20.2 ± 0.7	14.7 ± 0.3
TDN	19.2 ± 0.9	8.70 ± 0.34	75.2 ± 2.4	42.6 ± 1.8	152 ± 18	44.6 ± 0.5	125 ± 2	69.6 ± 1.8	219 ± 4	151 ± 3	139 ± 1	81.3 ± 9.6
vitispirane	36.3 ± 1.1	23.2 ± 0.3	89.8 ± 3.2	65.7 ± 1.5	83.7 ± 7.0	42.2 ± 0.1	80.7 ± 2.7	58.7 ± 1	120 ± 1	100 ± 1	83.1 ± 1.2	65.4 ± 4.1
α-terpineol	15.2 ± 0.1	16.4 ± 0.2	16.0 ± 0.2	16.6 ± 0.1	8.45 ± 0.25	7.25 ± 0.13	17.0 ± 0.3	18.8 ± 0.3	17.4 ± 0.2	21.3 ± 0.1	17.5 ± 0.1	20.6 ± 0.4
geraniol	0.573 ± 0.012	2.27 ± 0.02	0.757 ± 0.024	2.67 ± 0.10	0.351 ± 0.013	1.26 ± 0.01	0.653 ± 0.021	2.56 ± 0.03	0.509 ± 0.027	1.94 ± 0.03	0.466 ± 0.032	2.40 ± 0.03
linalool	1.60 ± 0.01	5.43 ± 0.10	2.21 ± 0.01	5.95 ± 0.08	2.22 ± 0.03	4.56 ± 0.07	3.18 ± 0.06	7.26 ± 0.02	2.36 ± 0.01	5.51 ± 0.02	2.48 ± 0.08	6.90 ± 0.10
linalool oxide	5.11 ± 0.08	3.12 ± 0.09	4.81 ± 0.21	3.97 ± 0.05	10.9 ± 0.4	6.22 ± 0.27	15.8 ± 0.4	11.1 ± 0.2	16.9 ± 0.2	12.8 ± 0.1	22.2 ± 0.1	17.1 ± 0.2
acetovanillone	17.9 ± 0.5	15.7 ± 0.3	16.8 ± 0.2	15.1 ± 0.2	31.6 ± 0.9	30.8 ± 0.9	21.0 ± 0.5	19.4 ± 0.2	36 ± 1	35.8 ± 0.6	31.5 ± 0.7	31.2 ± 0.2
vanillin	53.2 ± 0.7	46.8 ± 0.3	46.6 ± 0.5	41.8 ± 0.5	71.3 ± 0.8	71.8 ± 0.6	81.4 ± 0.6	79.6 ± 1.6	77.4 ± 7.0	86.1 ± 3.4	108 ± 1	104 ± 1
4-vinylguaiacol	10.2 ± 0.2	31.5 ± 0.3	9.24 ± 1.07	70.6 ± 1.6	79.8 ± 2.1	78.2 ± 2	21.3 ± 1.1	31.6 ± 3.6	50.9 ± 5.5	114 ± 1	27.7 ± 0.5	46.0 ± 1.6
4-vinylphenol	26.1 ± 3.6	93.2 ± 1.8	31.6 ± 3.2	238 ± 4	182 ± 1	235 ± 2	71.4 ± 2.7	113 ± 9	122 ± 16	297 ± 10	89.9 ± 5.6	171 ± 12
guaiacol	8.34 ± 0.18	3.41 ± 0.04	5.49 ± 0.06	3.48 ± 0.05	6.95 ± 0.37	3.24 ± 0.02	7.41 ± 0.31	3.84 ± 0.11	9.10 ± 0.09	5.84 ± 0.02	15.3 ± 0.2	9.03 ± 0.03
methoxyeugenol	1.45 ± 0.03	0.731 ± 0.031	1.16 ± 0.01	0.767 ± 0.03	1.49 ± 0.04	0.977 ± 0.045	1.11 ± 0.04	0.861 ± 0.007	2.00 ± 0.06	1.61 ± 0.04	2.03 ± 0.02	1.80 ± 0.002
syringol	112 ± 2	68.6 ± 0.1	83.1 ± 0.9	60.8 ± 2.2	124 ± 3	58.3 ± 0.6	110 ± 6	53.5 ± 0.4	88.2 ± 0.3	61.1 ± 0.6	129 ± 2	77.8 ± 0.1
eugenol	0.150 ± 0.005	0.145 ± 0.006	0.185 ± 0.004	0.173 ± 0.007	0.461 ± 0.022	0.456 ± 0.03	0.157 ± 0.008	0.162 ± 0.005	0.163 ± 0.005	0.203 ± 0.007	0.139 ± 0.007	0.151 ± 0.002
ethyl cinnamate	0.279 ± 0.013	0.182 ± 0.003	0.236 ± 0.011	0.198 ± 0.015	0.097 ± 0.004	0.0649 ± 0.0021	0.155 ± 0.006	0.104 ± 0.002	0.254 ± 0.014	0.189 ± 0.003	0.252 ± 0.008	0.281 ± 0.009

Table 2
Average concentrations and standard deviations (n = 2) of the aroma compounds (expressed in μg/L) evaluated at two different conditions (5 weeks at 50 °C and 24 h at 75 °C) in the 6 PAFs of Tempranillo (n.d: the compound was not detected).

Compounds	T1		T2		T3		T4		T5		T6	
	50 °C	75 °C	50 °C	75 °C	50 °C	75 °C	50 °C	75 °C	50 °C	75 °C	50 °C	75 °C
3-mercaptohexanol	1.17 ± 0.16	0.816 ± 0.018	2.44 ± 0.11	2.01 ± 0.04	1.07 ± 0.01	2.14 ± 0.04	1.03 ± 0.13	1.18 ± 0.03	4.59 ± 0.08	7.28 ± 0.15	3.87 ± 0.29	3.53 ± 0.02
isobutanal	0.815 ± 0.044	0.61 ± 0.01	1.09 ± 0.13	0.854 ± 0.031	1.15 ± 0.04	0.882 ± 0.016	1.73 ± 0.18	1.37 ± 0.05	2.10 ± 0.11	1.65 ± 0.08	1.95 ± 0.15	1.42 ± 0.06
2-methylbutanal	2.19 ± 0.09	1.42 ± 0.03	2.75 ± 0.15	1.59 ± 0.07	2.79 ± 0.03	1.78 ± 0.09	3.40 ± 0.10	2.21 ± 0.03	3.44 ± 0.26	2.77 ± 0.06	3.62 ± 0.23	2.24 ± 0.17
isovaleraldehyde	0.541 ± 0.026	0.773 ± 0.047	0.753 ± 0.022	0.958 ± 0.02	0.932 ± 0.002	1.45 ± 0.02	1.11 ± 0.04	2.35 ± 0.05	2.73 ± 0.08	3.29 ± 0.01	1.38 ± 0.06	1.72 ± 0.10
methional	1.44 ± 0.05	1.56 ± 0.01	1.18 ± 0.02	1.48 ± 0.07	1.24 ± 0.06	1.52 ± 0.05	1.60 ± 0.02	1.38 ± 0.07	1.44 ± 0.06	1.66 ± 0.06	1.10 ± 0.04	1.48 ± 0.06
phenylacetaldehyde	n.d.	1.76 ± 0.07	n.d.	1.78 ± 0.04	n.d.	2.23 ± 0.01	n.d.	2.21 ± 0.01	1.65 ± 0.03	4.15 ± 0.02	n.d.	1.78 ± 0.01
γ-nonalactone	0.507 ± 0.005	0.438 ± 0.029	0.676 ± 0.021	0.614 ± 0.042	0.535 ± 0.057	0.526 ± 0.001	0.732 ± 0.076	0.729 ± 0.019	0.744 ± 0.047	0.708 ± 0.007	1.76 ± 0.06	1.57 ± 0.06
massoia lactone	3.51 ± 0.02	3.03 ± 0.01	3.27 ± 0.05	2.63 ± 0.19	3.75 ± 0.09	3.04 ± 0.02	4.28 ± 0.10	3.29 ± 0.01	3.13 ± 0.04	2.22 ± 0.06	13.3 ± 0.2	9.76 ± 0.34
β-damascenone	9.09 ± 0.15	10.7 ± 0.5	10.1 ± 0.1	12.3 ± 0.5	5.09 ± 0.33	6.14 ± 0.04	5.23 ± 0.12	5.3 ± 0.2	7.82 ± 0.11	8.81 ± 0.09	6.99 ± 0.07	6.09 ± 0.21
Riesling acetal	5.80 ± 0.06	3.29 ± 0.04	9.10 ± 0.16	6.71 ± 0.24	7.74 ± 0.33	6.65 ± 0.04	8.81 ± 0.13	4.31 ± 0.19	27.6 ± 0.4	20.0 ± 0.7	11.5 ± 0.2	5.40 ± 0.65
TDN	18.3 ± 2.1	7.31 ± 0.40	18.0 ± 0.3	12.3 ± 1.0	14.7 ± 0.5	14.7 ± 0.3	19.8 ± 0.3	4.08 ± 0.27	85.3 ± 2.1	49.8 ± 0.4	26.2 ± 0.6	7.71 ± 0.63
vitispirane	41.3 ± 2.8	24.6 ± 0.3	54.7 ± 0.9	45.4 ± 4.5	40.2 ± 2.4	43.6 ± 0.2	45.9 ± 1.8	19.6 ± 0.3	100 ± 2	89.5 ± 0.4	63.2 ± 0.2	31.0 ± 2.5
α-terpineol	2.99 ± 0.01	2.40 ± 0.05	3.49 ± 0.07	3.42 ± 0.33	4.00 ± 0.07	4.87 ± 0.06	4.11 ± 0.07	3.31 ± 0.08	20.9 ± 0.1	23.2 ± 0.5	3.77 ± 0.04	2.49 ± 0.14
geraniol	n.d.	0.429 ± 0.016	n.d.	0.452 ± 0.009	n.d.	0.44 ± 0.01	n.d.	0.444 ± 0.01	0.580 ± 0.072	2.14 ± 0.03	n.d.	0.431 ± 0.018
linalool	0.434 ± 0.012	1.24 ± 0.02	0.565 ± 0.029	1.39 ± 0.09	0.589 ± 0.006	1.22 ± 0.02	0.692 ± 0.011	1.36 ± 0.06	1.85 ± 0.16	5.38 ± 0.04	0.670 ± 0.032	1.48 ± 0.05
linalool oxide	2.57 ± 0.05	1.20 ± 0,02	2.05 ± 0.03	1.44 ± 0.12	2.23 ± 0.11	2.03 ± 0.01	2.61 ± 0.08	1.05 ± 0.04	5.58 ± 0.01	4.12 ± 0.09	3.21 ± 0.04	1.29 ± 0.09
acetovanillone	17.1 ± 0.2	15.6 ± 0.1	26.1 ± 0.2	24.7 ± 0.1	14.2 ± 0.1	13.2 ± 0.1	18.0 ± 0.2	16.5 ± 0.7	56.0 ± 0.6	52.1 ± 0.6	23.1 ± 0.1	21.2 ± 0.4
vanillin	84.5 ± 0.6	87.3 ± 0.4	78.9 ± 2.0	77.5 ± 2.8	99.5 ± 8.2	118 ± 1	139 ± 3	152 ± 1	208 ± 2	205 ± 8	135 ± 5	151 ± 4
4-vinylguaiacol	7.01 ± 0.19	1.84 ± 0.10	3.25 ± 0.15	2.08 ± 0.1	8.28 ± 0.96	1.62 ± 0.06	4.11 ± 0.10	1.9 ± 0.2	38.4 ± 4.7	5.90 ± 0.13	5.65 ± 0.08	2.40 ± 0.29
4-vinylphenol	92.9 ± 4.8	7.52 ± 0.33	30.2 ± 3.5	7.51 ± 0.4	69.0 ± 6.7	9.04 ± 0.97	34.7 ± 0.8	8.84 ± 0.34	81.4 ± 4.0	18.6 ± 0.1	39.5 ± 1.6	9.07 ± 1.27
guaiacol	9.28 ± 0.02	4.91 ± 0.02	11.1 ± 0.1	7.97 ± 0.17	8.57 ± 0.51	6.52 ± 0.01	13.5 ± 0.3	7.90 ± 0.25	11.1 ± 0.4	6.93 ± 0.22	13.0 ± 0.3	6.63 ± 0.09
methoxyeugenol	4.57 ± 0.10	2.69 ± 0.12	9.22 ± 0.93	7.20 ± 0.29	3.92 ± 0.03	3.41 ± 0.05	4.97 ± 0.1	2.64 ± 0.01	3.18 ± 0.05	2.18 ± 0.03	7.86 ± 0.02	4.37 ± 0.14
syringol	205 ± 3	111 ± 1	177 ± 1	124 ± 2	168 ± 5	125 ± 1	212 ± 1	126 ± 3	111 ± 4	67.7 ± 1.1	160 ± 1	80.8 ± 0.9
eugenol	0.44 ± 0.01	0.395 ± 0.015	1.08 ± 0.03	1.07 ± 0.04	0.591 ± 0.036	0.613 ± 0.005	0.590 ± 0.023	0.487 ± 0.006	0.214 ± 0.006	0.204 ± 0.012	0.621 ± 0.002	0.511 ± 0.029
ethyl cinnamate	0.147 ± 0.008	0.0321 ± 0.0017	0.156 ± 0.010	0.107 ± 0.006	0.117 ± 0.003	0.0356 ± 0.0004	0.173 ± 0.008	0.11 ± 0.01	0.257 ± 0.013	0.145 ± 0.007	0.175 ± 0.005	0.105 ± 0.005

phenylacetaldehyde were also found in the hydrolysates. Phenylacetaldehyde have been detected previously in acid hydrolysates (Alegre, Sáenz-Navajas, et al., 2020; Loscos et al., 2009), which is consistent with our findings, although the origin of these molecules in these types of samples is not clear. In any case, excluding methional, Strecker aldehyde levels were significantly higher in Grenache hydrolysates, which confirms recent results regarding the higher tendency of this variety to accumulate Strecker aldehydes (Bueno-Aventín et al., 2021).

On the other hand, the PCA plot shows that the type of hydrolysis dominated the second component, with samples obtained by mild hydrolysis at 50 °C in the upper part of the plot, and those obtained at 75 °C in the lower part. As can be seen, the conditions used in the assay at 75 °C led to higher levels of MH, Riesling acetal, TDN, vitispirane, guaiacol, methoxyeugenol and syringol, while conditions used at 50 °C, produced higher levels of terpenols and Strecker aldehydes.

These results are supported by the ANOVA study to assess the effects of the hydrolysis and of the grape variety shown in Table S3 of the supplementary material. The hydrolysis factor was only significant for 12 out of the 25 compounds determined, while variety was significant in all cases except methional.

Most remarkably, the geographical distribution of samples differing only in the hydrolysis type is basically similar in all cases, as can be seen in the plot. For instance, equivalent samples from tempranillo (coded with T) have approximately the same coordinate in the PC1, the difference being that samples hydrolyzed at 75 °C have scores in PC2, 2 to 3 units smaller than those hydrolyzed at 50 °C. Similarly, all equivalent samples from grenache (coded with G) hydrolyzed at 50 °C have scores in PC1, just 0.5–1 units smaller than those hydrolyzed at 75 °C, which in all cases have scores in PC2, 3 to 4 units smaller. This clearly indicates that the type of hydrolysis does not essentially change relative differences between samples, particularly if these are from the same variety.

3.2.2. *Correlation between fast and mild hydrolysis*

In general terms, very good and significant correlations between

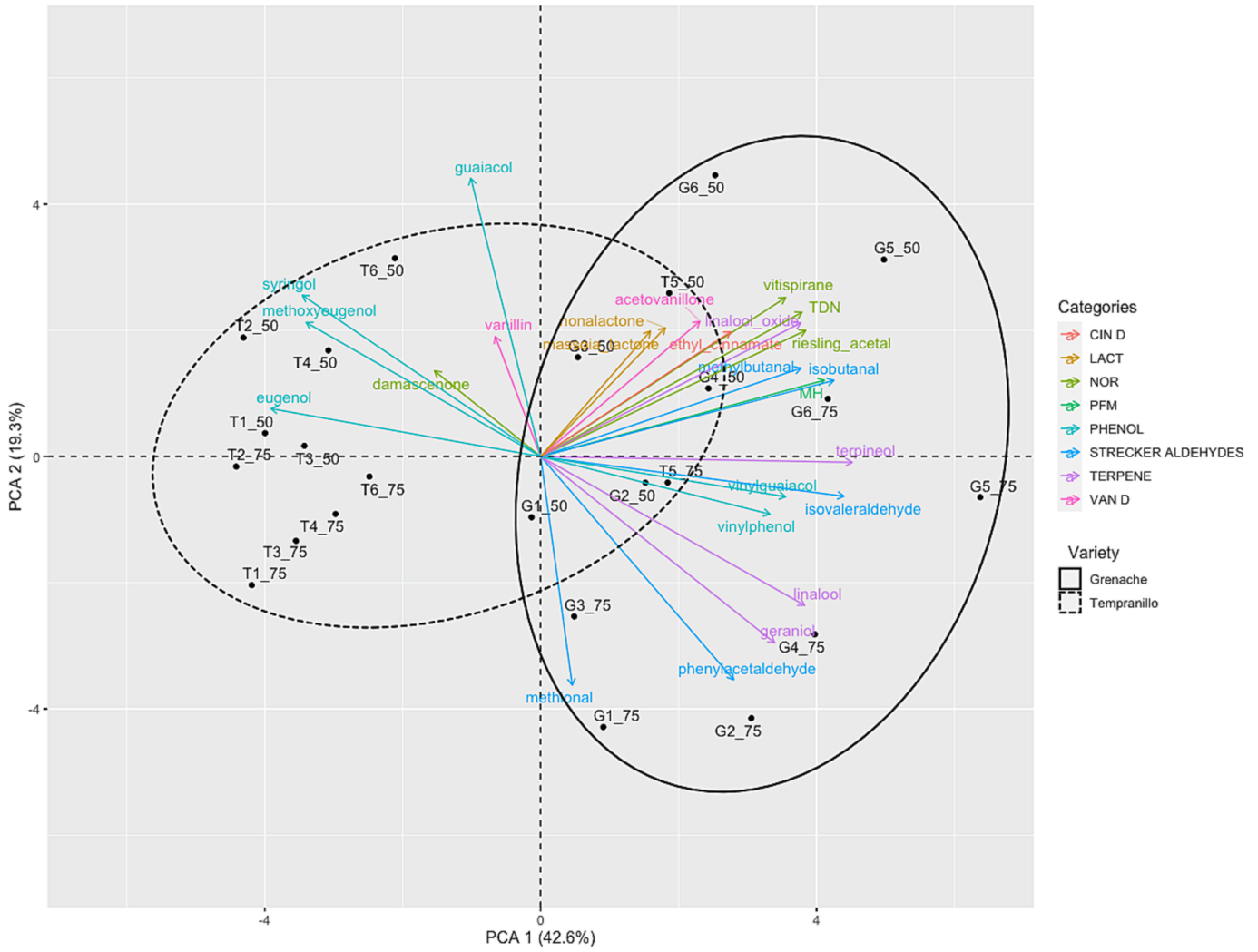

Fig. 4. Projection of samples and variables in the PCA plane obtained from the first two principal components. Samples for each hydrolysis conditions are indicate by the appendix "_50" or "_75" corresponding to mild hydrolysis (50 °C for 5 weeks) or fast hydrolysis (75 °C for 24 h) respectively. The categories are: CIN D (cinnamic derivates), LACT (lactones), NOR (norisoprenoids), PFM (polyfunctional mercaptans), PHENOL (volatile phenols), STRECKER ALDEHYDES, TERPENE (terpenes), VAN D (vanillin derivates).

both types of acid hydrolysis were observed, with coefficients of determination (R^2) higher than 0.9 in 13 compounds, and higher than 0.7 in the other 8 cases, as can be seen in Table S4. Among terpenoids, the best correlations were found for α-terpineol ($R^2 = 0.9849$) and linalool oxide ($R^2 = 0.9814$), both end-products of the degradation of terpenols. This was expected since in both types of hydrolysis the hydrolysis time, chosen as a compromise, was much longer than the time at which the maxima levels of the two most relevant terpenes, linalool and geraniol, are observed (Fig. 1). In spite of this, the correlation for geraniol was high ($R^2 = 0.9626$). Confirming the temperature effects observed in Fig. 1, the levels of α-terpineol were markedly higher at 75 °C, consistent with a higher degradation of linalool and other non-quantified monoterpenols (Maicas & Mateo, 2005). Most remarkably, when correlating the concentration of α-terpineol produced at 75 °C with the sum of α-terpineol released at 50 °C plus the difference of linalool concentrations at both temperatures, the slope of the correlation curve obtained was 1, supporting that linalool was mostly transformed into α-terpineol.

Regarding norisoprenoids, data confirmed that β-damascenone and Riesling acetal were well correlated, while TDN and vitispirane were less correlated than the others. These results just confirmed that the hydrolysis time chosen at 75 °C as a compromise (24 h) was too short to obtain a good development of TDN and vitispirane.

Some volatile phenols, such as eugenol and methoxyeugenol, could also be satisfactorily predicted by using a fast hydrolysis procedure. However, guaiacol could be only poorly predicted, surely also because hydrolysis time at 75 °C was too short for this compound. Finally, as expected given the complicated evolutions observed in the first part of this work, the levels of 4-vinylphenol and 4-vinylguaiacol could not be satisfactorily predicted from data at 75 °C. By contrast, vanillin derivatives, except syringol, could be most adequately predicted, as shown in Table S4.

Massoia lactone and γ-nonalactone were well predicted by hydrolysis at 75 °C; however, their range of variation was very short, except one sample (G6) with much higher levels of both lactones, particularly of massoia lactone, which could suggest that the grapes of this sample had suffered dehydration (Ferreira & Lopez, 2019).

In the case of aldehydes, levels found at 50 °C were in some cases too low to be reliably quantified, which explained why only isovaleraldehyde, isobutanal and phenylacetaldehyde showed significant correlations, while methional and 2-methybutanal were not correlated.

Finally, among varietal thiols, the powerful odorant 3-mercaptohexanol, was produced in similar quantities under both hydrolysis conditions, confirming its production from PAFs at mild hydrolysis, as previously reported (Alegre, Arias-Pérez, et al., 2020). Levels of MH

released after 5 weeks at 50 °C were well correlated with those obtained by fast hydrolysis after 24 h, which confirms the validity of the assay to predict the release of this important odorant from PAFs.

4. Conclusions

Models based on first-order kinetics seem to be appropriate for interpreting the accumulation of aroma molecules derived from the hydrolysis of precursors, also including those aroma molecules that further suffer degradation.

The study carried out at three different temperatures has made it possible to classify aroma molecules derived from specific precursor molecules present in grapes into three categories attending to the stability of both the aroma molecule and of the precursor: labile molecules from labile precursors, stable molecules from labile precursors and stable molecules from stable precursors.

For many grape-derived aroma molecules, the patterns of accumulation at the three temperatures were quite similar, levels accumulated were also similar, and on average, the reactions rates increased by factors 6.9 and 72 when temperature was increased from 35 to 50 or 75 °C, respectively. The Arrhenius-like plot has made it possible to estimate that for most aroma compounds, fast hydrolysis at 75 °C was 460 times faster than that observed at 20 °C. A clear exception to this pattern were vinylphenols and 3-mercaptohexanol, which hardly accumulated at 35 °C, suggesting that their hydrolyses had very high activation energies. TDN, vitispirane and α-terpineol were also more accumulated at higher temperatures.

Despite these differences, a study carried out with 12 different samples hydrolyzed at 50 °C for 5 weeks and at 75 °C for 24 h confirmed that fast hydrolysis adequately reproduced varietal and between-sample aroma compositional differences, and that the accumulated levels of 21 relevant grape-derived aroma compounds were highly correlated to those at 50 °C, so that fast hydrolysis can be safely used to predict grape aroma potential.

CRediT authorship contribution statement

Elayma Sánchez-Acevedo: Methodology, Formal analysis, Investigation, Resources, Data curation, Writing – review & editing, Visualization. **Ricardo Lopez:** Formal analysis, Writing – original draft, Writing – review & editing, Supervision, Project administration. **Vicente Ferreira:** Conceptualization, Formal analysis, Writing – original draft, Writing – review & editing, Visualization, Supervision, Project administration, Funding acquisition.

Declaration of Competing Interest

The authors declare that they have no known competing financial interests or personal relationships that could have appeared to influence the work reported in this paper.

Data availability

Data will be made available on request.

Acknowledgements

This work was funded by the Spanish Ministry of Science and Innovation (MICIN) (project AGL2017-87373-C3-1-R). Elayma Sánchez-Acevedo has received a grant (PRE2018-084968) from the Spanish FPI programs associated to the same project. LAAE acknowledges the continuous support of Gobierno de Aragón (T29) and European Social Fund.

Appendix A. Supplementary material

Supplementary data to this article can be found online at https://doi.org/10.1016/j.foodchem.2023.137935.

References

Alegre, Y., Arias-Pérez, I., Hernández-Orte, P., & Ferreira, V. (2020). Development of a new strategy for studying the aroma potential of winemaking grapes through the accelerated hydrolysis of phenolic and aromatic fractions (PAFs). *Food Research International, 127*, Article 108728. https://doi.org/10.1016/j.foodres.2019.108728

Alegre, Y., Sáenz-Navajas, M. P., Hernández-Orte, P., & Ferreira, V. (2020). Sensory, olfactometric and chemical characterization of the aroma potential of Garnacha and Tempranillo winemaking grapes. *Food Chemistry, 331*, Article 127207. https://doi.org/10.1016/j.foodchem.2020.127207

Bakker, J., & Clarke, R. J. (2011). *Wine: Flavour chemistry*. John Wiley & Sons.

Bonnaffoux, H., Delpech, S., Rémond, E., Schneider, R., Roland, A., & Cavelier, F. (2018). Revisiting the evaluation strategy of varietal thiol biogenesis. *Food Chemistry, 268*, 126–133. https://doi.org/10.1016/j.foodchem.2018.06.061

Bueno-Aventín, E., Escudero, A., Fernández-Zurbano, P., & Ferreira, V. (2021). Role of Grape-Extractable Polyphenols in the Generation of Strecker Aldehydes and in the Instability of Polyfunctional Mercaptans during Model Wine Oxidation. *Journal of Agricultural and Food Chemistry, 69*(50), 15290–15300. https://doi.org/10.1021/acs.jafc.1c05880

Carlin, S., Lotti, C., Correggi, L., Mattivi, F., Arapitsas, P., & Vrhovšek, U. (2022). Measurement of the Effect of Accelerated Aging on the Aromatic Compounds of Gewürztraminer and Teroldego Wines, Using a SPE-GC-MS/MS Protocol. *Metabolites, 12*(2), 180. https://doi.org/10.3390/metabo12020180

Castejón-Musulén, O., Manuel Aragón-Capone, A., Ontañón, I., Peña, C., Ferreira, V., & Bueno, M. (2022). Accurate quantitative determination of the total amounts of Strecker aldehydes contained in wine. Assessment of their presence in table wines. *Food Research International, 162, Part B*, 112125. Doi: 10.1016/j.foodres.2022.112125.

Cho, J. Y., Kim, S. J., Lee, H. J., & Moon, J. H. (2014). Two novel glycosyl cinnamic and benzoic acids from korean black raspberry (Rubus coreanus) wine. *Food Science and Biotechnology, 23*(4), 1081–1085. https://doi.org/10.1007/S10068-014-0148-7

Cibaka, M.-L.-K., Tran, T. T. H., Gros, J., Robiette, R., & Collin, S. (2017). Investigation of 2-Sulfanylethyl Acetate Cysteine- S -Conjugate as a Potential Precursor of Free Thiols in Beer. *Journal of the American Society of Brewing Chemists, 75*(3), 228–235. https://doi.org/10.1094/ASBCJ-2017-3276-01

Coulter, A., Baldock, G., Parker, M., Hayasaka, Y., Francis, I. L., & Herderich, M. (2022). Concentration of smoke marker compounds in non-smoke-exposed grapes and wine in Australia. *Australian Journal of Grape and Wine Research, 28*(3), 459–474. https://doi.org/10.1111/ajgw.12543

Daniel, M. A., Puglisi, C. J., Capone, D. L., Elsey, G. M., & Sefton, M. A. (2008). Rationalizing the formation of damascenone: Synthesis and hydrolysis of damascenone precursors and their analogues, in both aglycone and glycoconjugate forms. *Journal of Agricultural and Food Chemistry, 56*(19), 9183–9189. https://doi.org/10.1021/jf8018134

Denat, M., Ontañón, I., Querol, A., & Ferreira, V. (2022). The diverse effects of yeast on the aroma of non-sulfite added white wines throughout aging. *LWT, 158*, Article 113111. https://doi.org/10.1016/j.lwt.2022.113111

Ferreira, V., & Lopez, R. (2019). The actual and potential aroma of winemaking grapes. *Biomolecules, 9*(12), 818. https://doi.org/10.3390/biom9120818

Ferreira, V., Ortín, N., Escudero, A., López, R., & Cacho, J. (2002). Chemical Characterization of the Aroma of Grenache Rosé Wines: Aroma Extract Dilution Analysis, Quantitative Determination, and Sensory Reconstitution Studies. *Journal of Agricultural and Food Chemistry, 50*(14), 4048–4054. https://doi.org/10.1021/jf0115645

Francis, I. L., Sefton, M. A., & Williams, P. J. (1992). Sensory descriptive analysis of the aroma of hydrolysed precursor fractions from semillon, chardonnay and sauvignon blanc grape juices. *Journal of the Science of Food and Agriculture, 59*(4), 511–520. https://doi.org/10.1002/jsfa.2740590414

Hampel, D., Robinson, A. L., Johnson, A. J., & Ebeler, S. E. (2014). Direct hydrolysis and analysis of glycosidically bound aroma compounds in grapes and wines: Comparison of hydrolysis conditions and sample preparation methods. *Australian Journal of Grape and Wine Research, 20*(3), 361–377. https://doi.org/10.1111/ajgw.12087

Hayasaka, Y., Dungey, K. A., Baldock, G. A., Kennison, K. R., & Wilkinson, K. L. (2010). Identification of a beta-D-glucopyranoside precursor to guaiacol in grape juice following grapevine exposure to smoke. *Analytica Chimica Acta, 660*(1–2), 143–148. https://doi.org/10.1016/J.ACA.2009.10.039

Hayasaka, Y., Wilkinson, K. L., Elsey, G. M., Raunkjær, M., & Sefton, M. A. (2007). Identification of Natural Oak Lactone Precursors in Extracts of American and French Oak Woods by Liquid Chromatography-Tandem Mass Spectrometry. *Journal of Agricultural and Food Chemistry, 55*(22), 9195–9201. https://doi.org/10.1021/JF072171U

Hillebrand, S., Schwarz, M., & Winterhalter, P. (2004). Characterization of anthocyanins and pyranoanthocyanins from blood orange [Citrus sinensis (L.) Osbeck] juice. *Journal of Agricultural and Food Chemistry, 52*(24), 7331–7338. https://doi.org/10.1021/jf0487957

Hjelmeland, A. K., & Ebeler, S. E. (2015). Glycosidically bound volatile aroma compounds in grapes and wine: A review. *American Journal of Enology and Viticulture, 66*(1), 1–11. https://doi.org/10.5344/ajev.2014.14104

Ibarz, M. J., Ferreira, V., Hernández-Orte, P., Loscos, N., & Cacho, J. (2006). Optimization and evaluation of a procedure for the gas chromatographic-mass spectrometric analysis of the aromas generated by fast acid hydrolysis of flavor precursors extracted from grapes. *Journal of Chromatography A, 1116*(1–2), 217–229. https://doi.org/10.1016/j.chroma.2006.03.020

López, R., Aznar, M., Cacho, J., & Ferreira, V. (2002). Determination of minor and trace volatile compounds in wine by solid-phase extraction and gas chromatography with mass spectrometric detection. *Journal of Chromatography A, 966*(1–2), 167–177. https://doi.org/10.1016/S0021-9673(02)00696-9

López, R., Ezpeleta, E., Sánchez, I., Cacho, J., & Ferreira, V. (2004). Analysis of the aroma intensities of volatile compounds released from mild acid hydrolysates of odourless precursors extracted from Tempranillo and Grenache grapes using gas chromatography-olfactometry. *Food Chemistry, 88*(1), 95–103. https://doi.org/10.1016/j.foodchem.2004.01.025

Loscos, N., Hernández-Orte, P., Cacho, J., & Ferreira, V. (2009). Comparison of the suitability of different hydrolytic strategies to predict aroma potential of different grape varieties. *Journal of Agricultural and Food Chemistry, 57*(6), 2468–2480. https://doi.org/10.1021/jf803256e

Maicas, S., & Mateo, J. J. (2005). Hydrolysis of terpenyl glycosides in grape juice and other fruit juices: A review. *Applied Microbiology and Biotechnology, 67*(3), 322–335. https://doi.org/10.1007/s00253-004-1806-0

Naim, M., Wainish, S., Zehavi, U., Peleg, H., Rouseff, R. L., & Nagy, S. (1993). Inhibition by Thiol Compounds of Off-Flavor Formation in Stored Orange Juice. 1. Effect of l-Cysteine and N-Acetyl-l-cysteine on 2,5-Dimethyl-4-hydroxy-3(2H)-furanone Formation. *Journal of Agricultural and Food Chemistry, 41*(9), 1355–1358. https://doi.org/10.1021/jf00033a002

Oliveira, I., & Ferreira, V. (2019). Modulating Fermentative, Varietal and Aging Aromas of Wine Using non- Saccharomyces Yeasts in a Sequential Inoculation Approach. *Microorganisms, 7*(6), 1–23. https://doi.org/10.3390/microorganisms7060164

Schievano, E., D'Ambrosio, M., Mazzaretto, I., Ferrarini, R., Magno, F., Mammi, S., & Favaro, G. (2013). Identification of wine aroma precursors in Moscato Giallo grape juice: A nuclear magnetic resonance and liquid chromatography-mass spectrometry tandem study. *Talanta, 116*, 841–851. https://doi.org/10.1016/j.talanta.2013.07.049

Schneider, R., Razungles, A., Augier, C., & Baumes, R. (2001). Monoterpenic and norisoprenoidic glycoconjugates of Vitis vinifera L. cv. Melon B. as precursors of odorants in Muscadet wines. *Journal of Chromatography A, 936*(1–2), 145–157. https://doi.org/10.1016/S0021-9673(01)01150-5

Sefton, M. A., Skouroumounis, G. K., Elsey, G. M., & Taylor, D. K. (2011). Occurrence, sensory impact, formation, and fate of damascenone in grapes, wines, and other foods and beverages. *Journal of Agricultural and Food Chemistry, 59*(18), 9717–9746. https://doi.org/10.1021/jf201450q

Segurel, M. A., Razungles, A. J., Riou, C., Trigueiro, M. G. L., & Baumes, R. L. (2005). Ability of possible DMS precursors to release DMS during wine aging and in the conditions of heat-alkaline treatment. *Journal of Agricultural and Food Chemistry, 53*(7), 2637–2645. https://doi.org/10.1021/jf048273r

Singh, D. P., Chong, H. H., Pitt, K. M., Cleary, M., Dokoozlian, N. K., & Downey, M. O. (2011). Guaiacol and 4-methylguaiacol accumulate in wines made from smoke-affected fruit because of hydrolysis of their conjugates. *Australian Journal of Grape and Wine Research, 17*(2), S13–S21. https://doi.org/10.1111/J.1755-0238.2011.00128.X

Slaghenaufi, D., & Ugliano, M. (2018). Norisoprenoids, sesquiterpenes and terpenoids content of Valpolicella wines during aging: Investigating aroma potential in relationship to evolution of tobacco and balsamic aroma in aged wine. *Frontiers in Chemistry, 6*, 66. https://doi.org/10.3389/fchem.2018.00066

Strauss, C. R., Dimitriadis, E., Wilson, B., & Williams, P. J. (1986). Studies on the Hydrolysis of Two Megastigma-3,6,9-triols Rationalizing the Origins of Some Volatile C13 Norisoprenoids of Vitis vinifera Grapes. *Journal of Agricultural and Food Chemistry, 34*(1), 145–149. https://doi.org/10.1021/jf00067a039

Tambawala, H., Batra, S., Shirapure, Y., & More, A. P. (2022). Curcumin- A Bio-based Precursor for Smart and Active Food Packaging Systems: A Review. *Journal of Polymers and the Environment, 30*(6), 2177–2208. https://doi.org/10.1007/s10924-022-02372-x

Tominaga, T., & Peyrot des Gachons, C., & Dubourdieu, D.. (1998). A New Type of Flavor Precursors in *Vitis v inifera* L. cv. Sauvignon Blanc: *S* -Cysteine Conjugates. *Journal of Agricultural and Food Chemistry, 46*(12), 5215–5219. https://doi.org/10.1021/jf980481u

Vázquez-Pateiro, I., Arias-González, U., Mirás-Avalos, J. M., & Falqué, E. (2020). Evolution of the Aroma of Treixadura Wines during Bottle Aging. *Foods, 9*(10), 1419. https://doi.org/10.3390/foods9101419

Vichi, S., Cortés-Francisco, N., & Caixach, J. (2015). Analysis of volatile thiols in alcoholic beverages by simultaneous derivatization/extraction and liquid chromatography-high resolution mass spectrometry. *Food Chemistry, 175*, 401–408. https://doi.org/10.1016/j.foodchem.2014.11.095

Wilkinson, K. L., Prida, A., & Hayasaka, Y. (2013). Role of glycoconjugates of 3-methyl-4-hydroxyoctanoic acid in the evolution of oak lactone in wine during oak maturation. *Journal of Agricultural and Food Chemistry, 61*(18), 4411–4416. https://doi.org/10.1021/jf400175h

Williams, P. J., Sefton, M. A., & Wilson, B. (1989). *Nonvolatile Conjugates of Secondary Metabolites as Precursors of Varietal Grape Flavor Components* (pp. 35–48). Doi: 10.1021/bk-1989-0388.ch004.

Williams, P. J., Strauss, C. R., & Wilson, B. (1980). Hydroxylated Linalool Derivatives as Precursors of Volatile Monoterpenes of Muscat Grapes. *Journal of Agricultural and Food Chemistry, 28*(4), 766–771. https://doi.org/10.1021/jf60230a037